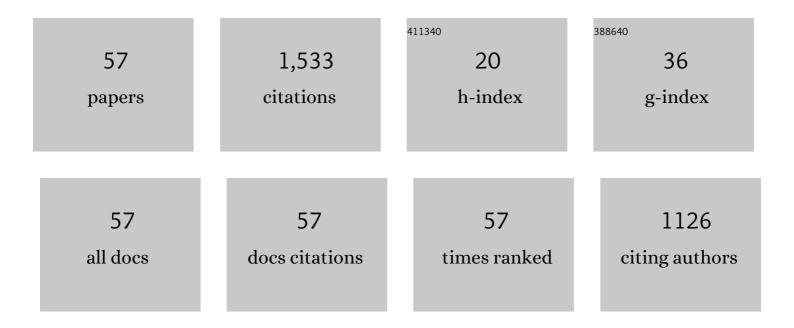
List of Publications by Year in descending order

Source: https://exaly.com/author-pdf/8833151/publications.pdf Version: 2024-02-01



#	Article	IF	CITATIONS
1	Collaborative enhancement of luminous efficacy and fracture toughness based on interface design of Al2O3/YAG:Ce3+ eutectic phosphor ceramic grown by laser floating zone melting. Ceramics International, 2022, 48, 10144-10154.	2.3	3
2	Temperature Field Evolution of Seeding during Directional Solidification of Single-Crystal Ni-Based Superalloy Castings. Metals, 2022, 12, 817.	1.0	2
3	Effect of withdrawal rate on precipitation characteristics of MC-type carbides in a nickel-based directionally solidified superalloy with high Re content. Vacuum, 2021, 183, 109800.	1.6	7
4	The effects of misfit and diffusivity on γʹ rafting in Re and Ru containing Nickel based single crystal superalloys—details in thermodynamics and dynamics. Vacuum, 2021, 183, 109839.	1.6	12
5	Investigation of the 12 orientations variants of nanoscale Al precipitates in eutectic Si of Al-7Si-0.6Mg alloy. Journal of Materials Science and Technology, 2021, 67, 186-196.	5.6	13
6	The Element Segregation Between γ/γʹ Phases in a Ni-Based Single Crystal Superalloy Studied by 3D-APT and Its Potential Impact on Local Interfacial Misfit Strain. Metals and Materials International, 2021, 27, 1892-1896.	1.8	12
7	Solidification characteristics and as-cast microstructures of a Ru-containing nickel-based single crystal superalloy. Journal of Materials Research and Technology, 2021, 11, 474-486.	2.6	22
8	Different roles of stacking fault energy and diffusivity in the creep performance of nickel-based single-crystal superalloys. Materials Research Express, 2021, 8, 036510.	0.8	0
9	Microstructure on remelting interface of Ni–W heterogeneous seed in preparing Ni-based single crystal superalloys. Journal of Materials Research and Technology, 2021, 12, 264-270.	2.6	3
10	Effect of substituting Mo for W on γ/γ′ partitioning behaviors of alloying elements in heat-treated second generation Ni based single crystal superalloys: An atom probe tomography study. Intermetallics, 2021, 134, 107198.	1.8	16
11	Peritectic reaction during directional solidification in a Ru-containing nickel-based single crystal superalloy. Journal of Alloys and Compounds, 2021, 870, 159419.	2.8	9
12	Formation mechanisms and control method for stray grains at melt-back region of Ni-based single crystal seed. Progress in Natural Science: Materials International, 2021, 31, 624-632.	1.8	6
13	Enhanced age-hardening by synergistic strengthening from Mg Si and Mg Zn precipitates in Al-Mg-Si alloy with Zn addition. Materials Characterization, 2020, 169, 110579.	1.9	10
14	Investigation on solution heat treatment response and γ′ solvus temperature of a Mo-rich second generation Ni based single crystal superalloy. Intermetallics, 2020, 125, 106896.	1.8	13
15	Effect of alloying elements on stacking fault energies of γ and γʹ phases in Ni-based superalloy calculated by first principles. Vacuum, 2020, 181, 109682.	1.6	34
16	Precipitation behavior and chemical composition of secondary γâ€> precipitates in a Re-containing Ni-based single crystal superalloy. Intermetallics, 2020, 119, 106725.	1.8	15
17	Effect of aging temperature on the secondary γ′ precipitation in a model Ni based single crystal superalloy. Journal of Alloys and Compounds, 2020, 836, 155486.	2.8	16
18	Inhibition of stray grains at melt-back region for re-using seed to prepare Ni-based single crystal superalloys. Progress in Natural Science: Materials International, 2019, 29, 582-586.	1.8	3

#	Article	IF	CITATIONS
19	Formation of Accumulated Misorientation During Directional Solidification of Ni-Based Single-Crystal Superalloys. Metallurgical and Materials Transactions A: Physical Metallurgy and Materials Science, 2019, 50, 1607-1610.	1.1	19
20	Dendrite growth and defects formation with increasing withdrawal rates in the rejoined platforms of Ni-based single crystal superalloys. Vacuum, 2019, 161, 29-36.	1.6	21
21	Orientation controlling of Ni-based single-crystal superalloy by a novel method: grain selection assisted by un-melted reused seed. Journal of Materials Research and Technology, 2019, 8, 1347-1352.	2.6	11
22	Formation of low-angle grain boundaries under different solidification conditions in the rejoined platforms of Ni-based single crystal superalloys. Journal of Materials Research, 2019, 34, 251-260.	1.2	17
23	Stress dependence of the creep behaviors and mechanisms of a third-generation Ni-based single crystal superalloy. Journal of Materials Science and Technology, 2019, 35, 752-763.	5.6	45
24	Formation of Lateral Sliver Defects in the Platform Region of Single-Crystal Superalloy Turbine Blades. Metallurgical and Materials Transactions A: Physical Metallurgy and Materials Science, 2019, 50, 1119-1124.	1.1	14
25	The role of vacuum degree in the bonding of Al/Mg bimetal prepared by a compound casting process. Journal of Materials Processing Technology, 2019, 265, 112-121.	3.1	42
26	Stress dependence of dislocation networks in elevated temperature creep of a Ni-based single crystal superalloy. Materials Science & Engineering A: Structural Materials: Properties, Microstructure and Processing, 2019, 742, 132-137.	2.6	27
27	Influence of Secondary Dendrite Orientation on the Evolution of Misorientation in the Platform Region of Single Crystal Superalloy Turbine Blades. Advanced Engineering Materials, 2019, 21, 1800933.	1.6	10
28	Negative influence of rafted γ′ phases on 750 °C/750 MPa creep in a Ni-based single crystal superalloy 4% Re addition. Materials Characterization, 2018, 137, 127-132.	with 1.9	16
29	Competitive converging dendrites growth depended on dendrite spacing distribution of Ni-based bi-crystal superalloys. Journal of Alloys and Compounds, 2018, 735, 1878-1884.	2.8	12
30	Nucleation Crystallography of Ni Grains on CrFeNb Inoculants Investigated by Edgeâ€ŧoâ€Edge Matching Model in an IN718 Superalloy. Advanced Engineering Materials, 2018, 20, 1700568.	1.6	10
31	Insight of the dendrite deformation in Ni-based superalloys for increased misorientation along convergent boundaries. Progress in Natural Science: Materials International, 2018, 28, 489-495.	1.8	15
32	Formation of Slivers in the Extended Crossâ€Section Platforms of Niâ€Based Single Crystal Superalloy. Advanced Engineering Materials, 2018, 20, 1701189.	1.6	15
33	Abnormal Grain Refinement Behavior in High-Pressure Die Casting of Pure Mg with Addition of Zr as Grain Refiner. Jom, 2018, 70, 2555-2560.	0.9	4
34	Effect of Zn Concentration on the Microstructure and Mechanical Properties of Al-Mg-Si-Zn Alloys Processed by Gravity Die Casting. Metallurgical and Materials Transactions A: Physical Metallurgy and Materials Science, 2018, 49, 3247-3256.	1.1	20
35	Halo formation of Zn-Al alloys under conventional solidification and intensive convection solidification. Journal of Alloys and Compounds, 2017, 696, 460-469.	2.8	6
36	Effect of secondary dendrite orientations on competitive growth of converging dendrites of Ni-based bi-crystal superalloys. Materials Characterization, 2017, 125, 152-159.	1.9	22

#	Article	IF	CITATIONS
37	Influence of withdrawal rate on the porosity in a third-generation Ni-based single crystal superalloy. Progress in Natural Science: Materials International, 2017, 27, 236-243.	1.8	17
38	Investigation on solidification path of Ni-based single crystal superalloys with different Ru contents. Materials Characterization, 2017, 130, 211-218.	1.9	17
39	Investigation on a ramp solution heat treatment for a third generation nickel-based single crystal superalloy. Journal of Alloys and Compounds, 2017, 723, 922-929.	2.8	16
40	Insight into the partial solutionisation of a high pressure die-cast Al-Mg-Zn-Si alloy for mechanical property enhancement. Materials Science & Engineering A: Structural Materials: Properties, Microstructure and Processing, 2017, 682, 85-89.	2.6	10
41	Effect of Co on microstructural stability of the third generation Ni-based single crystal superalloys. Journal of Materials Research, 2016, 31, 1328-1337.	1.2	22
42	Enhanced Grain Refinement and Porosity Control of the Polycrystalline Superalloy by a Modified Thermally Controlled Solidification. Advanced Engineering Materials, 2016, 18, 1785-1791.	1.6	9
43	Solid-liquid interface and growth rate range of Al2O3-based eutectic in situ composites grown by laser floating zone melting. Journal of Alloys and Compounds, 2016, 662, 634-639.	2.8	26
44	Heterogeneous nucleation in Mg–Zr alloy under die casting condition. Materials Letters, 2015, 160, 263-267.	1.3	23
45	Effect of Mg level on the microstructure and mechanical properties of die-cast Al–Si–Cu alloys. Materials Science & Engineering A: Structural Materials: Properties, Microstructure and Processing, 2015, 642, 340-350.	2.6	66
46	Melt superheating on the microstructure and mechanical properties of diecast Al-Mg-Si-Mn alloy. Metals and Materials International, 2015, 21, 382-390.	1.8	14
47	Investigation of mechanical and corrosion properties of an Al–Zn–Mg–Cu alloy under various ageing conditions and interface analysis of Î-′ precipitate. Materials and Design, 2015, 85, 752-761.	3.3	116
48	Effect of solutionising and ageing on the microstructure and mechanical properties of a high strength die-cast Al–Mg–Zn–Si alloy. Materials Chemistry and Physics, 2015, 167, 88-96.	2.0	19
49	Grain boundary precipitation induced by grain crystallographic misorientations in an extruded Al–Mg–Si–Cu alloy. Journal of Alloys and Compounds, 2015, 624, 27-30.	2.8	37
50	Initial precipitation and hardening mechanism during non-isothermal aging in an Al–Mg–Si–Cu 6005A alloy. Materials Characterization, 2014, 94, 170-177.	1.9	31
51	Heterogeneous Nucleation of α-Al Grain on Primary α-AlFeMnSi Intermetallic Investigated Using 3D SEM Ultramicrotomy and HRTEM. Metallurgical and Materials Transactions A: Physical Metallurgy and Materials Science, 2014, 45, 3971-3980.	1.1	30
52	Precipitation behaviour of Al–Zn–Mg–Cu alloy and diffraction analysis from η′ precipitates in four variants. Journal of Alloys and Compounds, 2014, 610, 623-629.	2.8	129
53	Effect of iron on the microstructure and mechanical property of Al–Mg–Si–Mn and Al–Mg–Si diecast alloys. Materials Science & Engineering A: Structural Materials: Properties, Microstructure and Processing, 2013, 564, 130-139.	2.6	231
54	Electron microscopy studies of the age-hardening behaviors in 6005A alloy and microstructural characterizations of precipitates. Journal of Alloys and Compounds, 2012, 514, 220-233.	2.8	56

#	Article	IF	CITATIONS
55	Precipitate characteristics and selected area diffraction patterns of the β′ and Q′ precipitates in Al–Mg–Si–Cu alloys. Philosophical Magazine Letters, 2011, 91, 150-160.	0.5	26
56	Studies of Orientations of β″ Precipitates in Al-Mg-Si-(Cu) Alloys by Electron Diffraction and Transition Matrix Analysis. Metallurgical and Materials Transactions A: Physical Metallurgy and Materials Science, 2011, 42, 2917-2929.	1.1	27
57	The diffraction patterns from β″ precipitates in 12 orientations in Al–Mg–Si alloy. Scripta Materialia, 2010, 62, 705-708.	2.6	89